Addressing Neon Gas Field Ion Source Instability Through Online Beam Current Estimation

Sheila W. Seidel[1,3*], Luisa Watkins[1], Minxu Peng[1], Akshay Agarwal[2], Christopher Yu[3], and Vivek K Goyal[1]

[1.] Boston University, Department of Electrical and Computer Engineering, Boston, MA, United States.
[2.] Massachusetts Institute of Technology, Department of Electrical and Computer Engineering, Cambridge, MA, United States.
[3.] Charles Stark Draper Laboratory, Cambridge, MA, United States.
* Corresponding author: SSeidel@bu.edu

Focused ion beam microscopes require stable beam current for accurate micrograph formation and sample milling. In practice, the beam current emitted by a gas field ion source may fluctuate away from the desired setting due to contamination. The neon beam microscope in particular has been less widely adopted due to poor temporal stability and shorter source lifetime. In a neon beam microscope, beam current variations may be modeled as jumping among a set of values, as shown for a set of two values in Figure 1(a) [1]. When a sample is raster scanned horizontally, these variations give rise to horizontal stripe artifacts in the micrograph, as shown in Figure 1(d). Existing microscopes do not measure the beam current, however mitigation techniques have been developed to remove horizontal content from micrographs post-facto [2]. These methods require tuning and can remove horizontal sample features in addition to the targeted artifacts. In [3,4], we showed that the time-resolved (TR) processing methods introduced in [5,6] greatly reduce the artifacts that arise due to imperfectly known beam current. In this work, we demonstrate online estimation of the unknown neon beam current from the same secondary electron count data used to form the micrograph [7]. Our beam current estimate further improves the micrograph and could also be used to prevent sample damage, improve milling accuracy, and for instrument diagnostics.

The number of incident ions at the kth pixel may be modeled as a Poisson random variable with mean $\lambda_k = \Lambda_k t$, where Λ_k is the rate of incident particles over time. The number of secondary electrons (SE) detected in response to each incident particle may also be modeled as a Poisson random variable with mean η_k. Here η_k is the 'SE yield', a material property we seek to recover when forming a micrograph. Assuming direct SE detection, a conventional microscope measures Y_k, the total number of SEs observed at the kth pixel over dwell time t. The conventional estimate of the micrograph (i.e., the secondary electron yield η_k) operates independently at each pixel: $\hat{\eta}_k^{\text{baseline}}(\tilde{\lambda}_k) = Y_k/\tilde{\lambda}_k$, assuming a beam current of $\tilde{\lambda}_k$. When this assumption is violated, error propagates into $\hat{\eta}_k^{\text{baseline}}$, giving rise to the stripes seen in Figure 1(d).

Time-resolved measurement divides dwell time t into n equally spaced sub-acquisitions, each with dose λ_k/n, and measures vector $\mathbf{Y}_k = [Y_k^{(1)}, Y_k^{(2)}, \cdots, Y_k^{(n)}]$ at the kth pixel. Time-resolved estimates of η combine these n measurements to estimate η at each pixel. For example, the time-resolved maximum likelihood (TRML) estimator $\hat{\eta}_k^{\text{TRML}}(\tilde{\lambda}_k)$ introduced in [5] and [6] returns the estimate of η that maximizes the likelihood of measurement $\mathbf{Y}_k$, given assumed beam current value $\tilde{\lambda}_k$. When beam current is perfectly known (i.e. $\tilde{\lambda}_k = \lambda_k$), time-resolved methods have been shown to greatly mitigate

the effects of source shot noise [5, 6]. Additionally, when beam current is imperfectly known, time-resolved estimation methods exhibit a natural robustness to striped artifacts [3, 4].

In this work, we model neon beam current as a two-state hidden Markov chain; our methods may be readily extended to more complicated discrete models, and continuous models are considered in [7]. The nature of the beam current variation is assumed to be well characterized so that states $\mathbf{s} \in \{s_1, s_2\}$ and transition probabilities between subsequent pixels $q(s, r) \coloneqq P(\lambda_{k+1} = s \,|\, \lambda_k = r)$ are known. We denote the mean beam current by $\bar{\lambda}$. Our *causal* (i.e. only using data from previously scanned pixels) joint estimation algorithm $(\hat{\eta}_k^C, \hat{\lambda}_k^C)$ applies TRML to form an initial estimate of η, assuming the beam current is $\tilde{\lambda}_k = \bar{\lambda}$ at each pixel: $\eta_k \approx \hat{\eta}_k^{\text{TRML}}(\tilde{\lambda}_k = \bar{\lambda})$. Given this assumed η, the Forward algorithm [8] is applied to compute the belief state $F_k(s) \coloneqq P(\lambda_k = s \mid \mathbf{Y}_{1:k})$ of λ_k given data from all previous pixels $\mathbf{Y}_{1:k}$. Our beam current estimate $\hat{\lambda}_k^C$ is chosen to be the state that maximizes the belief state $F_k(s)$. We apply TRML a second time, assuming the beam current is $\tilde{\lambda} = \hat{\lambda}_k^C$, to form our estimate of SE yield: $\hat{\eta}_k^C = \hat{\eta}_k^{\text{TRML}}(\tilde{\lambda}_k = \hat{\lambda}_k^C)$. A similar *non-causal* estimate $(\hat{\eta}_k^{\text{NC}}, \hat{\lambda}_k^{\text{NC}})$ is designed to operate on *all* sample data, after the full scan is complete.

In Figure 1, we show results from a synthetic neon beam experiment and compare estimator root-mean square error (RMSE). The beam current time series, Figure 1(a), was generated according to a two-state Markov chain model with $\lambda \in \{20, 30\}$ using transition probabilities $P(\lambda_k = 20 \,|\, \lambda_{k-1} = 30) = 0.003$ and $P(\lambda_k = 30 \,|\, \lambda_{k-1} = 20) = 0.002$. At each pixel, the dwell time is divided into $n = 300$ time-resolved sub-acquisitions. The conventional estimate in Figure 1(d) exhibits prominent stripe artifacts. In Figure 1(b) we plot the "Oracle" TRML estimate, formed with perfect knowledge of the beam current (i.e., $\tilde{\lambda}_k = \lambda_k$), and in Figure 1(e) we plot TRML estimate formed using only the mean beam current (i.e., $\tilde{\lambda} = \bar{\lambda}$). Note that, as seen in [3, 4], the RMSE of the TRML method with $\tilde{\lambda} = \bar{\lambda}$ is substantially smaller than the conventional method, with small additional gains with oracular knowledge of the beam current. Hidden Markov model-based causal $\hat{\eta}_k^C$ (Figure 1(c)) and non-causal $\hat{\eta}_k^{\text{NC}}$ (Figure 1(f)) estimates achieve even lower RMSE with performance approaching the Oracle method. The non-causal estimate, which considers all scan data post-facto, performs slightly better.

In Figure 2, we plot our causal $\hat{\lambda}^C$ and non-causal $\hat{\lambda}^{\text{NC}}$ beam current estimates alongside the ground truth λ time series. The causal estimate exhibits an extremely close match to the ground truth, with the incorrect state selected 0.77% of the time. The non-causal estimate, which has the advantage of considering all scan data, has an even lower error rate of 0.13%. In addition to improving the underlying micrograph, we have demonstrated accurate estimate of the beam current. This knowledge of the beam current could improve milling outcomes, prevent sample damage, and extend the useable source lifetime making neon beam microscopy more accessible [9].
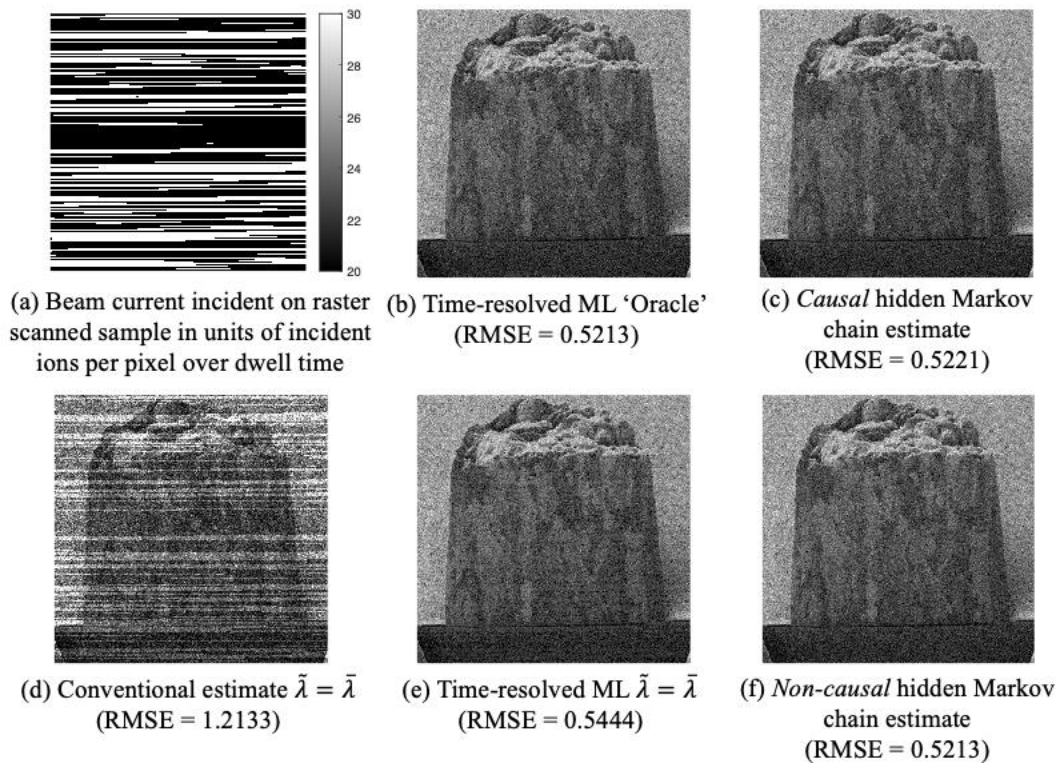
Figure 1. Results from a synthetic experiment with η ∈ [2, 6], n=300, and λ modeled as a two-state hidden Markov chain with λ ∈ {20, 30} as shown in (a). Root-mean square error (RMSE) is marked for each case.
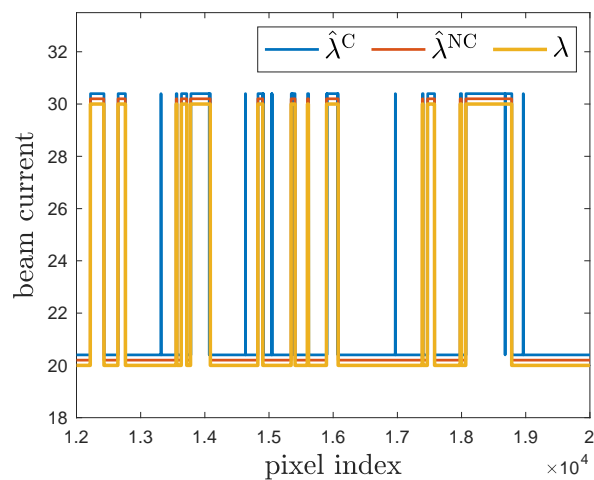
Figure 2. Causal $\hat{\lambda}^{C}$ and non-causal $\hat{\lambda}^{NC}$ beam current estimates at a subset of pixels plotted with ground truth λ. Error rate is 0.77% for causal algorithm and 0.13% for non-causal algorithm. Small vertical offsets introduced to increase legibility.

References:

[1] J. Notte et al., Microsc. Microanal. **16**(S2) (2010), p. 28.

[2] A. J. Barlow et al., Microsc. Microanal. **22**(5) (2016), p. 939.

[3] L. Watkins et al., Proc. IEEE Int. Conf. Image Process., Anchorage, AK, Sep. 2021, p. 3487.

[4] L. Watkins et al., Microsc. Microanal. **27**(S1) (2021), p. 422.

[5]. M. Peng et al., Ultramicroscopy **211** (2020), p. 112948.

[6] M. Peng, J. Murray-Bruce, and V. K. Goyal, IEEE Trans. Computational Imaging **7** (2021), pp. 547.

[7] S. W. Seidel et al., arXiv:2111.10611 (2021).

[8] L. E. Baum, Inequalities **3**(1) (1972).

[9] The authors acknowledge funding by a Draper Fellowship, a Boston University Clare Boothe Luce Scholar Award and by the US National Science Foundation under Grant No. 1815896.